Journal of Bioscience and Bioengineering
VOL. 128 No. 6, 755–765, 2019

ELSEVIER

www.elsevier.com/locate/jbiosc

Cloning, identification and functional characterization of two cytochrome P450 carotenoids hydroxylases from the diatom *Phaeodactylum tricornutum*

Hongli Cui,[1,‡] Haotian Ma,[1,‡] Yulin Cui,[2] Xiaoli Zhu,[1] Song Qin,[2] and Runzhi Li[1,*]

Institute of Molecular Agriculture and Bioenergy, Shanxi Agricultural University, Taigu 030801, China[1] *and Key Laboratory of Coastal Biology and Biological Resources Utilization, Yantai Institute of Coastal Zone Research, Chinese Academy of Sciences, Yantai 264003, China*[2]

Received 13 March 2019; accepted 11 June 2019
Available online 2 July 2019

The diatom microalgal *Phaeodactylum tricornutum* accumulates a large amount of fucoxanthin. Carotenoids hydroxylases (CHYs) play key roles in fucoxanthin biosynthesis in diatoms. However, not any type of CHYs had been identified in *P. tricornutum*. In this study, two genes (designated *Ptrcyp97b1* and *Ptrcyp97b2*) were cloned, identified and functionally characterized. They shared high sequence identity (50–94 %) with lutein deficient 1-like proteins from other eukaryotes. The typical catalytic active motifs of cytochrome P450s (CYP) were detected in the amino acid sequences of PtrCYP97B1 and PtrCYP97B2. The two genes were probably due to gene duplication. *Ptrcyp97b1* and *Ptrcyp97b2* transcriptional expression was up-regulated with distinct patterns under high light conditions. The metabolic profiles of the major carotenoids (β-carotene, zeaxanthin, diadinoxanthin, diatoxanthin and fucoxanthin) were determined based on the high performance liquid chromatography method. The fucoxanthin and diatoxanthin contents were increased, while the β-carotene content was decreased. By truncation of the N-terminal trans-membrane anchor or chloroplast transit peptide and addition of a 6 × His-tag, PtrCYP97B1 and PtrCYP97B2 were separately heterologously produced in *Escherichia coli* and purified by Ni-NTA affinity chromatography. Functional analysis showed that PrtCYP97B2 was able to catalyze the hydroxylation of the β-rings of β-carotene to produce zeaxanthin in β-carotene-accumulating *E. coli* BL21(DE3) cells. PtrCYP97B1 might have the ability to catalyze the hydroxylation of other substrates other than β-carotene. These results contribute to the further elucidation of xanthophyll biosynthesis in diatoms.

[**Key words:** Cytochrome P450; Carotenoids hydroxylase; *Phaeodactylum tricornutum*; Cloning; Identification; Functional characterization]

Microalgae are important potential sources of diverse carotenoids which are divided into two major groups that include carotenes (Cars) and xanthophylls (Xans). Cars are enriched in the center of the photosystem reaction. Xans are oxygenated Cars that serve various functions in photosynthetic organisms and are essential for the survival of the organism (1–3). Fucoxanthin (Fcx), diadinoxanthin (Ddx) and diatoxanthin (Dtx) are the most abundant and special Xans (contributing more than 10 %) in the marine environment and reveal remarkable biological properties with many applications (4). For instance, Fcx is a significant component of Fcx-chlorophyll-protein-complexes (FCPs) that are functionally related to the light-harvesting-complexes (LHCs) of green microalgae and higher plants. Fcx acts as an antenna and transfers excitation energy to chlorophyll *a*/*c*. The light induced conversion of Dtx and Ddx protects the organisms from photodamage (5). Fcx is also a safe kind of Xan that is absorbable and exhibits various biological and physiological activities in the human gut (6–11). Therefore, seeking good sources of natural Fcx has recently attracted much attention. Fortunately, some previous studies have demonstrated that *Phaeodactylum tricornutum* is a rich source of Fcx (at least ten times more abundant than that in macroalgae) (12). In addition, the genome sequence of *P. tricornutum* (CCAP1055/1) is available (13). Molecular techniques based on transformation have been developed in recent years (14). Therefore, *P. tricornutum* is a perfect organism for investigating genes involved in Fcx biosynthesis.

Carotenoids hydroxylases (CHYs) are important enzymes involved in the hydroxylation reaction for α- and β-branch Xans biosynthesis in photosynthetic organisms. To date, four types of CHYs (named CrtR, BCH, CYP97A and CYP97C) have been identified and characterized by comparative genomics and functional biochemistry methods in cyanobacteria, eukaryotic microalgae and higher plants (2,15). In green microalgae and higher plants, two classes of structurally unrelated CHYs, including two heme-containing cytochrome P450s hydroxylases (CYP97A and CYP97C) and a pair of nonheme/di-iron hydroxylases (BCH1 and BCH2) have been identified (15–17). In cyanobacteria, CrtR catalyzes the hydroxylation of Cars (18). However, not any type of CHYs had been cloned from the diatom (2,3,19). Unlike CYP97A and CYP97C, the function of CYP97B in Xans biosynthesis remains poorly understood. In higher plants, it has been indicated that CYP97B might be able to hydroxylate the β-rings of β-carotene and α-carotene, as observed in *Arabidopsis* (20). However, in the quadruple mutant (*bch1*, *bch2*, *cyp97c1* and *cyp97a3*) that contained only CYP97B3, Xans did not accumulate, indicating that CYP97B might not be an

* Corresponding author. Tel./fax: +86 354 628 8344.
E-mail addresses: cuihongli2005@163.com (H. Cui), mht_sxau@163.com (H. Ma), yulincui@yic.ac.cn (Y. Cui), fenfang56@126.com (X. Zhu), sqin@yic.ac.cn (S. Qin), rli2001@126.com (R. Li).
‡ The first two authors contributed equally to this work.

1389-1723/$ – see front matter
https://doi.org/10.1016/j.jbiosc.2019.06.008

important enzyme for carotene hydroxylation (21). In microalgae, it has been implied that CYP97B (PuCHY1) from red algae (*Porphyra*) might be able to hydroxylate the β-rings of β-carotene to produce zeaxanthin (22).

At present, three hypothetical pathways for Fcx biosynthesis in diatoms have been proposed and discussed (Fig. S1). First, the neoxanthin (Nex) is produced from β-carotene (β-Car) through intermediate metabolites that include in turn, zeaxanthin (Zea), antheraxanthin (Atx) and violaxanthin (Vlx). Then neoxanthin, as the branch point, is converted to Fcx or Ddx (3). The first synthetic pathway is summarized as follows, β-Car→Zea→Atx→Vlx→Nex→Fcx or Ddx. Second, the Vlx is produced from β-Car through intermediate metabolites that include in turn, Zea and Atx. Then Vlx is converted into Ddx, which is further transformed into Fcx or Dtx (23). The second synthetic pathway is summarized as follows, β-Car→Zea→Atx→Vlx→ Ddx→Fcx or Dtx. Finally, Vlx is synthesized from β-Car through intermediate metabolites that include in turn, β-cryptoxanthin (β-Cpx) and β-cryptoxanthin-5,6-epoxide. Then Vlx is converted to Ddx which is further transformed into Fcx or Dtx (19). The finally synthetic pathway is summarized as follows, β-Car→β-Cpx→β-Cpx-5,6-epoxide→Vlx→Ddx→Fcx or Dtx. However, for the three pathways described, the genes encoding the CHYs responsible for the hydroxylation of β-Car into Zea or β-Cpx are missing to date.

Previous studies have shown that the gene encoding β-carotene hydroxylase (BCH), which is responsible for the hydroxylation of β-Car, is absent in the *P. tricornutum* CCAP1055/1 genome, and only a partial sequence is present in the *T. pseudonana* CCMP 1335 genome (3,23). Fortunately, studies have indicated that LUT-like P450 proteins may be responsible for the hydroxylation of Cars in diatoms (23). The discovery of P450-type monooxygenases (CYP97A and CYP97C) involved in carotenoid hydroxylation not only makes up the missing pieces of carotenoid biosynthetic enzymes but also provides valuable clues for detecting novel CHYs genes in diatoms (2,15). Moreover, previous results have implied that the homologs of *cyp97a* and *cyp97c* genes were widespread only in green microalgae, while *cyp97b* homologs were present in almost all microalgae including diatoms (2,23). In addition, two putative genes encoding CYP97Bs (LUT-like1 and LUT-like2) have been predicted in *P. tricornutum* CCAP1055/1 (2,23). However, there are not any reports on molecular cloning, sequence analysis, transcriptional expression and functional characterization of CYP97Bs in *P. tricornutum*. This study, therefore, aimed to identify and characterize genes encoding CYP97Bs in *P. tricornutum*. The transcriptional expression of *Ptrcyp97b* genes and the carotenoid composition of cells were investigated under different high light (HL) conditions. Moreover, two putative PtrCYP97Bs were separately heterologously produced, purified and functionally characterized in β-Car-accumulating *Escherichia coli* BL21(DE3) cells.

MATERIALS AND METHODS

Algal strain and culture conditions *P. tricornutum* strain GY-H9 was maintained in our laboratory and was cultivated in 100 mL f/2 liquid medium and placed in an illuminating incubator under light intensity of 75 μmol photons m^{-2} s^{-1}, with a photoperiod of 12 h/12 h (light/dark) at temperature of 25 ± 1°C. For the HL conditions, after the cultures were dark-adapted for 48 h, the later exponentially growing cultures (2 L and cell density of approximately 5 × 10^8 cells mL^{-1}) were further transferred into continuous white light (AHDGYB-5730-30-390-770, TTIUEIT, Beijing, China; 390–770 nm) or blue light (AHDGYB-5730-30-420-500, TTIUEIT; 420–500 nm) with a light intensity of 500 μmol photons m^{-2} s^{-1} without a light/dark cycle. The cultures under white light intensity of 75 μmol photons m^{-2} s^{-1} without a light/dark cycle were used as the control Samples were collected at the end of the dark period and after the onset of light by centrifugation and the cells were washed with PBS prior to storage in liquid nitrogen.

Molecular cloning of PtrCYP97B1 and PtrCYP97B2 cDNAs Total RNA was extracted from *P. tricornutum* GY-H9 cells using the TRIzol reagent (Takara, Dalian, China) according to the user's manual. In this protocol, RNA was treated with DNase I and quantified by NanoDrop 2000c (Thermo Fischer Scientific, Waltham, MA, USA). First-strand cDNAs were synthesized from 2 μg of total RNA with RT Enzyme Mix I Kit (Takara) according to the manufacturer's instructions. Two pairs of degenerate primers (Table S1: PtrCYP97B-F1/PtrCYP97B-R1 and PtrCYP97B-F2/PtrCYP97B-R2) for homologous cloning were designed by CODEHOP (http://diyhpl.us/~bryan/irc/protocol-online/protocol-cache/codehop.html) based on the highly conserved regions of putative genes encoding CYP97B or LUT-like proteins predicted from higher plants and microalgae (Table S2). First-strand cDNAs were used as a template. PCR amplification was conducted with LATaq Kit (Takara) according to the manufacturer's instructions, and the PCR was processed with the following parameters: initial denaturation at 94°C for 5 min followed by 35 cycles of 94°C for 30 s, 58°C (according to the Tm values of primers) for 30 s, and 72°C for 1 min (according to the length of products at 1000 bp min^{-1}), with a final extension at 72°C for 7 min and cooling to 4°C. The fragments of interest were purified and cloned into the pMD-18T vector (Takara) and sequenced (Invitrogen, Shanghai, China). The full-length cDNAs of *Ptrcyp97b1* and *Ptrcyp97b2* were amplified by the RACEs method according to the manual of the SMARTTM RACE cDNA Amplification Kit (Clontech, Palo Alto, CA, USA). The gene specific primers (Table S1: PtrCYP97B1-3-F1/PtrCYP97B1-3-F2, PtrCYP97B2-3-F1/PtrCYP97B2-3-F2, PtrCYP97B1-5-R1/PtrCYP97B1-5-R2 and PtrCYP97B2-5-R1/PtrCYP97B2-5-R2) were designed from the amplified core cDNAs sequences of *Ptrcyp97b1* and *Ptrcyp97b2*. Nested PCRs were carried out using the nested universal primers and gene specific primers. The ORFs of *Ptrcyp97b1* and *Ptrcyp97b2* were cloned by the primers (Table S1: PtrCYP97B1-C-F/PtrCYP97B1-C-R and PtrCYP97B2-C-F/PtrCYP97B2-C-R). The obtained nucleotide sequences corresponding to the complete open reading frames were submitted to the NCBI database with the accession numbers of MK955952 and MK955953.

Bioinformatics analysis The molecular weight (Mw), isoelectronic point (pI), sub-cellular localization, signal peptides, trans-membrane regions, secondary and tertiary structures of PtrCYP97B1 and PtrCYP97B2 were computed and predicted by ExPASy (https://www.expasy.org/) (24). PtrCYP97B proteins and others were aligned using ClustalX (25). Maximum likelihood trees (Le and Gascuel evolutionary model) of some CYP97 proteins were constructed using PhyML (26,27). Bootstrap (BS) values were inferred from 400 replicates.

Transcriptional analysis under HL conditions qRT-PCR was performed on an ABI fast 7500 Sequence Detection System (Applied Biosystems, Foster, CA, USA). qRT-PCR primers (Table S1: PtrCYP97B1-Q-F/PtrCYP97B1-Q-R and PtrCYP97B2-Q-F/PtrCYP97B2-Q-R) were used. The gene histone primers (Table S1: Ptrhistone-Q-F/Ptrhistone-Q-R) were selected as an internal control (23). The amplifications were carried out in triplicate in a total volume of 20 μL according to the manufacturer's instructions of SYBR Premix Ex Taq Kit (Takara). The program was holding stage, 50°C for 20 s and 95°C for 10 min, followed by 40 cycles of 95°C for 15 s, 60°C for 1 min, and melt curve stage, 95°C for 15 s, 60°C for 1 min, 95°C for 30 s, and 60°C for 15 s. DEPC-treated water for the replacement of template was used as negative control. The comparative CT method ($2^{-\Delta\Delta CT}$) was used to investigate the transcription expression of genes (28). The specific gene primers are listed in Supplementary Table S1 and were designed with Primer 5.0 software.

Carotenoids analysis under HL conditions For cell dry biomass determination, 40 mL cells culture was collected by centrifugation at 13,100 ×*g* at 4°C for 5 min and the collection of cells washed three times. The EP tubes containing cells were dried in a DW3 freeze-drier (Heto Dry Winner, Thermo Fisher Scientific, Shanghai, China). For carotenoids analysis, the high performance liquid chromatography (HPLC) method was applied to quantify the contents of all the carotenoids (16). Briefly, the freeze-dried cells (0.01 g) were ground with liquid nitrogen and extracted with acetone until the cells became colorless. After centrifugation at 13,100 ×*g* at 4°C for 15 min, the supernatant was collected and evaporated under nitrogen gas. Finally, the residue was re-dissolved in 1 mL acetone and filtered through a 0.22-mm Millipore organic membrane (Millipore Co., Burlington, MA, USA) prior to HPLC analysis. Carotenoids were eluted at a flow rate of 1.2 mL min^{-1} with a linear gradient from 100 % solvent A [acetonitrile/methanol/0.1 M Tris–HCl (84:2:14), pH 8.0] to 100 % solvent B [methanol/ethyl acetate (68:32)] for 15 min, followed by 12 min of solvent B. The absorption spectra of the carotenoids ranged from 300 nm to 700 nm (UltiMate 3000, Thermo Fisher Scientific). Peaks were measured at 450 nm. The contents of β-Car (PHR1239-1G, Sigma–Aldrich, St. Louis, MO, USA) [X = (Y − 62.67668)/132,194.37218], Zea (14681-1 MG-F, Sigma–Aldrich) [X = (Y + 30.38239)/228,228.27718], Ddx (08379-1 MG, Sigma–Aldrich) [X=(Y − 37.33045)/234,509.96862], Dtx (79449-1 MG, Sigma–Aldrich) [X = (Y + 15.45376)/345,607.56473] and Fcx (F6932-10 MG, Sigma–Aldrich) [X = (Y + 45.45235)/145,673.34516] were determined using the standard curves of standard carotenoids at known concentrations. The carotenoids standards were purchased from Sigma–Aldrich. In these above formulas, X is content of pigment (mg mL^{-1}) and Y is integration of the peak areas (450 nm).

Heterologous expression and purification of recombinant PtrCYP97Bs in *E. coli* cells *Ptrcyp97b1* and *Ptrcyp97b2* genes encoding only mature proteins were amplified using the following primers: PtrCYP97B1-28a-F/PtrCYP97B1-28a-R and PtrCYP97B2-28a-F/PtrCYP97B2-28a-R (Table S1). Both the sequenced products and the pET-28a(+) plasmid (P0023, Miaoling Bioscience & Technology Co., Ltd.,

Wuhan, China) were digested with *Eco*R I and *Xho* I and then ligated and further transformed into *E. coli* BL21(DE3) competent cells. Transformed *E. coli*-pET28a(+)-*Ptrcyp97b1* and *E. coli*-pET28a(+)-*Ptrcyp97b2* cells were separately grown at 37°C in LB medium containing 30 μg mL^{-1} kanamycin until the OD_{600} reached 0.4–0.6. Then, isopropyl β-D-thiogalactoside (IPTG) was added to a final concentration of 0.1 mM. Cultivation was continued at 18°C and 120 × g for 24 h. the cells were harvested by centrifugation (6000 ×*g* at 4°C for 10 min) and were re-suspended in 20 mM sodium phosphate buffer (containing 5 mM imidazole, 0.2 mg mL^{-1} lysozyme, 20 μg mL^{-1} DNase and 1 mM $MgCl_2$) and then disrupted by ultra-sonication. The supernatant was obtained by centrifugation (13,100 ×*g* at 4°C for 15 min). The recombinant proteins were purified by loading them into a Ni-Sepharose 6FF column (GE Healthcare, Piscataway, NJ, USA). His-tagged target proteins were eluted with imidazole at concentrations ranging from 50 to 300 mM in 20 mM sodium phosphate buffer. The purity and molecular weight of R-PtrCYP97B1 and R-PtrCYP97B2 were determined using 7 % (W V^{-1}) sodium dodecyl sulfate-polyacrylamide gel electrophoresis (SDS–PAGE). Protein bands on SDS–PAGE were visualized by staining with Coomassie Brilliant Blue R-250.

Functional characterization of PtrCYP97Bs in β-Car-producing *E. coli* cells In the present study, the recombinant plasmids pET28a(+)-*Ptrcyp97b1* and pET28a(+)-*Ptrcyp97b2* were separately transformed into the β-Car-accumulating (harboring pACCAR16ΔcrtX) *E. coli* BL21(DE3) cells (29). Transformed *E. coli*-pET28a(+)-*Ptrcyp97b1* and *E. coli*-pET28a(+)-*Ptrcyp97b2* cells were separately grown at 37°C in LB medium containing both 30 μg mL^{-1} kanamycin and 50 μg mL^{-1} chloramphenicol until the OD_{600} reached 0.4–0.6, respectively. After induction with 0.1 mM isopropyl β-D-1-thiogalactopyranoside (IPTG) (0487, Amresco, Shanghai, China) for 24 h at 18°C and 120 ×*g*, the carotenoids were extracted from the *E. coli* cells. For carotenoids analysis, the HPLC method was applied to quantify the content of each pigment (16). The contents of β-Car [X = (Y − 62.67668)/132,194.37218], β-Cpx (C6368-1 MG, Sigma–Aldrich) [X = (Y − 58.65247)/145,786.69847] and Zea [X = (Y + 30.38239)/228,228.27718] were determined using standard curves of the standard carotenoids at known concentrations.

Statistical analysis All exposure experiments were repeated independently three times, and data were recorded as the mean with standard deviation (SD). For gene expression experiments, the expression, measured as the mean ± SD (% control), was calculated using the (standard curve) approximation corrected for primer efficiency and normalized to the expression values of the housekeeping *histone* gene. Statistical analysis was performed with SPSS (version 19.0) statistical software. Data were considered significantly different at $P < 0.05$ or $P < 0.01$ (one-way ANOVA, Turkey HSD test).

RESULTS

Cloning and identification of two genes encoding PtrCYP97Bs Detailed information about the cDNA sequences of *Ptrcyp97b1* (MK955952) and *Ptrcyp97b2* (MK955953) is summarized in Table S3. The *Ptrcyp97b1* cDNA sequence was 2605 base pairs (bp) in length, which contained a 2268 bp open reading frame (ORF), a 220 bp 5′-untranslated region (UTR), and a 117 bp 3′-UTR with the characteristic of the poly(A) tail. The deduced protein had a calculated molecular weight of 85.26 kDa with an estimated isoelectric point of 5.25. The cloned *Ptrcyp97b2* cDNA was 2194 bp in length and contained an ORF of 1875-bp with a 5′-UTR of a 217-bp and 3′-UTR of 102-bp and encoded a protein of 624 amino acids. The deduced protein had a calculated molecular weight of 70.48 kDa with an estimated isoelectric point (pI) of 5.23.

A BLASTp (https://blast.ncbi.nlm.nih.gov) search revealed that PtrCYP97B1 and PtrCYP97B2 shared high sequences similarity (49–94 %) with some predicted lutein-deficient 1-like or CYP97B proteins from diatom, green microalgae and higher plants (Table S4). Analyses of the trans-membrane helices, chloroplast transit peptides and signal peptides suggested that PtrCYP97B1 might be a nuclear gene encoded and cytoplasm-targeted enzyme (Fig. S2 and Table S3). On the contrary, chloroplast transit peptides, but not trans-membrane helices were predicted in the amino acid sequence of PtrCYP97B2 (Fig. S3 and Table S3), which implied a soluble enzyme localized in the chloroplast. The distinct subcellular localization for different PtrCYP97Bs is consistent with the localization of PtrLUT-like1 and PtrLUT-like2 predicted from the genome sequences of *P. tricornutum* CCAP1055/1 (23).

The PtrCYP97Bs and other CYP97B or LUT-like proteins were aligned using the ClustalX program. These results revealed that eight conserved domains (CDs) were discovered in the amino acid sequences of PtrCYP97B1 and PtrCYP97B2 (Fig. 1), which is consistent with previous study (2,23). Briefly, the CYP450s active site components, e.g., CD4 (I-helix) involved in oxygen binding, CD5 (ERR triad) involved in locking the heme and assuring stabilization of the conserved core structure, and CD7 involved in heme binding were found. In addition, there were some CYP97B subfamily-specific CDs including YC/DKGM/VLAEIL, FGSV/IT-X-ESPI/VIKAVY-X4-EAEHRS, DPSLLRFLVD/GMRGE/AD and LYPS/NE-X3-DFAF.

The phylogenetic analysis of the CYP97s from eukaryotic microalgae and higher plants is illustrated in Fig. 2, which is also consistent with previous results (2). Briefly, the cloned PtrCYP97B1 and PtrCYP97B2 formed separate cluster (BS: 100/100) among those of other predicted LUT-like proteins from Bacillariophyta. The CYP97Bs and LUT-like proteins from Bacillariophyta constituted a monophyletic group (BS: 97), which further formed another monophyletic group (BS: 72) with CYP97Bs from green microalgae and higher plants as a sister group. Interestingly, gene encoding CYP97B from each organism of green microalgae and higher plants was single copy while genes encoding CYP97Bs or LUT-like proteins were double copies in each organism from Bacillariophyta. In particular, lineage-specific gene duplication event might occur during the evolution of CYP97Bs or LUT-like proteins in Bacillariophyta.

Transcriptional expression of *PtrCYP97*Bs under HL conditions Time-course transcriptional patterns of *Ptrcyp97b1* and *Ptrcyp97b2* in photoautotrophic *P. tricornutum* GY-H9 under different HL conditions were determined (Fig. 3). The transcriptional level of *Ptrcyp97b1* increased at 12–60 h exposure under blue HL and reached the maximum was measured at 36 h exposure, which was 5.84-fold higher than that of the control. A steady and strong increase of *Ptrcyp97b1* transcript level (2.48-fold higher than that of the control) at 24–60 h exposure was found under white HL condition (Fig. 3A). The transcript level of *Ptrcyp97b1* gene in both blue and white HL was similar, but the kinetics of increase were faster in blue HL than in white HL (Fig. 3A). We found a transitory and strong increase of *Ptrcyp97b2* transcript levels after 12–24 h of blue and white HL, and after this period the levels decreased again (Fig. 3B). As shown in Fig. 3B, the highest steady state transcript levels were measured after 12 h and reached approximately 5.02-fold and 4.75-fold higher under blue and white HL respectively than that of the control. Then it decreased sharply and remained relatively constant when exposure during 36–72 h under both blue and white HL conditions. The corresponding patterns of *Ptrcyp97b2* expression under blue and white HL conditions were essentially identical. The effect of blue HL on *Ptrcyp97b2* transcript level was stronger than white HL. Blue HL appeared to have a stronger effect on both *Ptrcyp97b2* and *Ptrcyp97b2* transcription than white HL, even though the response patterns were distinct.

Carotenoids accumulation of Xans under HL conditions The biomass yield and accumulation of β-Car, Zea, Ddx, Dtx and Fcx were examined over the period of induction (Fig. 4). The results implied that white HL condition slightly promoted growth during the (0–72 h) exposure, while blue HL condition mildly inhibited growth (Fig. 4A). In summary, different HL conditions had no obvious effect on growth and biomass yield. The later exponentially growing cultures were used for different HL conditions, which was responsible for the above phenomenon. Upon blue and white HL conditions, in the early stress induction (0–12 h), the content of β-Car decreased sharply and remained stable through the 12–72 h exposure, had a lower value than that of measured at control. The final β-Car content under blue HL was less than it was under white HL condition (Fig. 4B). It was interesting to mention that the Zea content increased rapidly and reached its maximum at 48 h and 36 h exposure under blue and

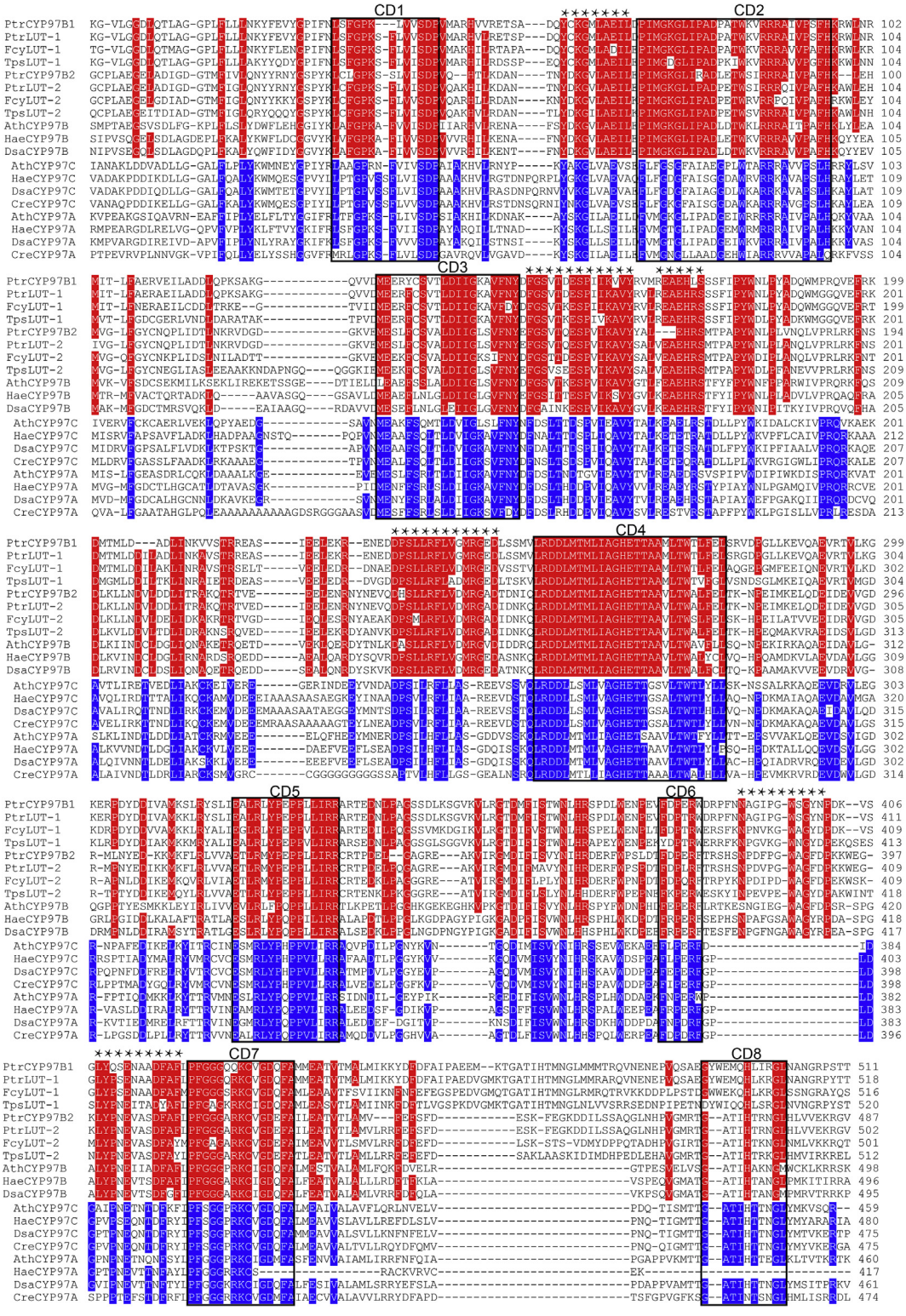

FIG. 1. Multiple alignments of CYP97 A/B/Cs. All the sequences information is summarized in Table S2. There are common eight conserved domains (black boxes: CD1-CD8) in the protein sequences of CYP97 A/B/Cs. The three typical conserved domains of all cytochrome P450s were discovered, including the oxygen binding site signature (CD4, LI/VAGHETT), the ERR triad involved in locking the heme (CD5, EXXRLYPXPPV/LLI/LRR), and the heme binding signature sequence (CD7, PFG/SGGPRKCXGDXFA). The CYP98B-specific CDs are indicated by black asterisks.

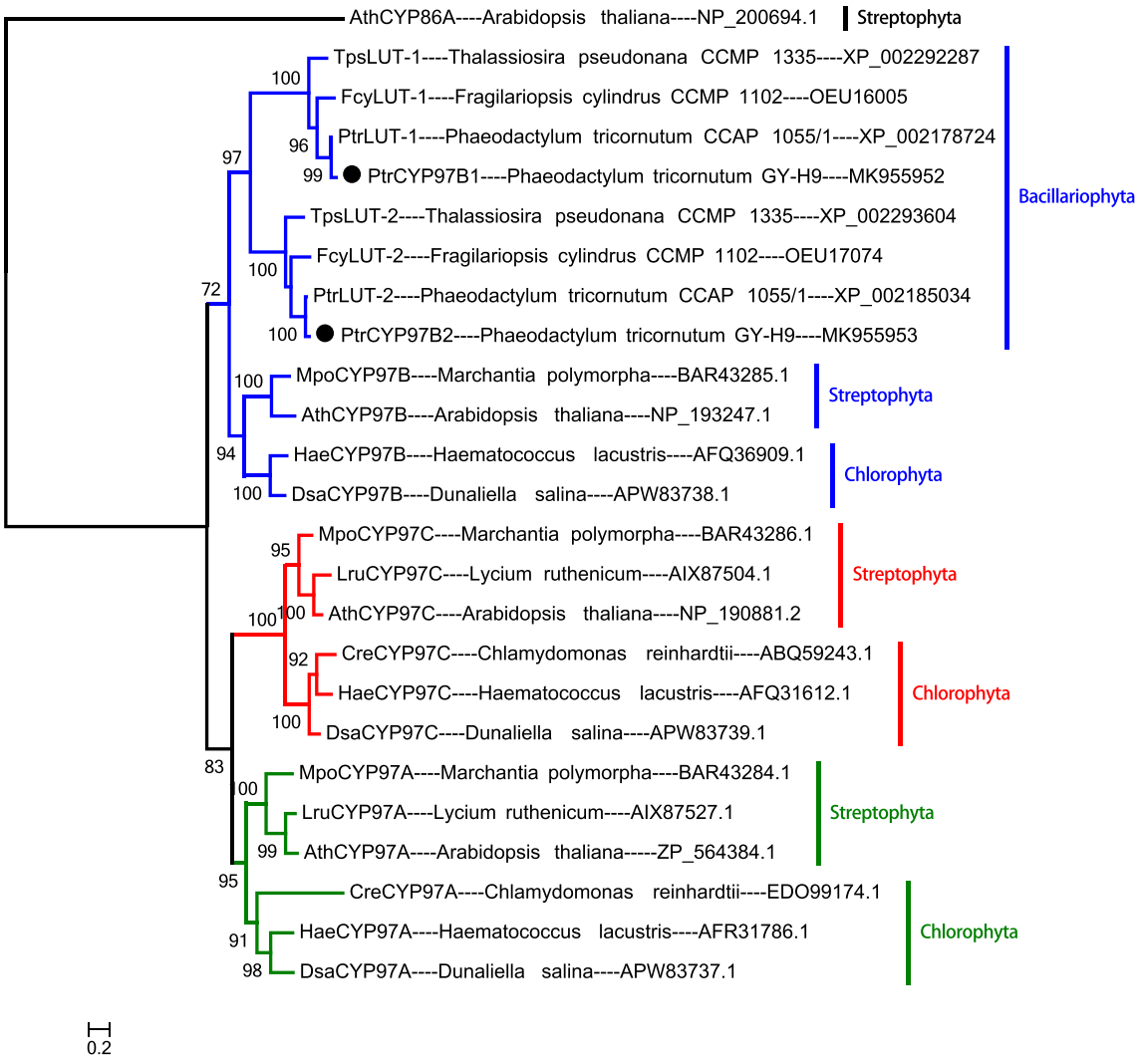

FIG. 2. Phylogenetic analysis of CYP97 A/B/Cs homologues from microalgae and higher plants. The maximum likelihood tree was constructed by PhyML software as described in Materials and methods. The sequences information of CYP97s from microalgae and higher plants is summarized in Table S2. A partial protein sequence (position: 270–910) has been selected for phylogenetic analysis. Numbers above branches indicate ML bootstrap supports. ML bootstraps were computed using the above model in 300 replicates. The PtrCYP97B1 and PtrCYP97B2 are indicated by black circles. Major groups of organisms are labeled to allow comparison between the phylogeny of CYP97 A/B/C and microalgae or higher plants evolution.

white HL conditions respectively. Then, it decreased sharply along the extension of induction (48–72 h), with the lower content value than that of measured at control (Fig. 4C). However, the content of Fcx under treatments increased markedly and reached the max values at 72 h exposure, which was higher than that of measured at control (Fig. 4D). The content of Ddx under treatment was relatively stable (Fig. 4E). In addition, the content of Dtx under both blue and white HL conditions increased slowly and reached its maximum at 72 h exposure (Fig. 4F). These above results suggested that compared with white HL, blue HL was more effective in inducing the synthesis of carotenoids in *P. tricornutum* GY-H9. These results also indicated that the coordinated up-regulation of *Ptrcyp97b1* and *Ptrcyp97b2* genes might give rise to a decrease in the content of the substrate (β-Car) and an increase in the contents of the major products (Fcx and Dtx) generated through the intermediate metabolite (Zea).

Heterologous expression of PtrCYP97Bs in *E. coli* BL21(DE3) cells To further characterize the catalytic properties of PtrCYP97Bs, the genes were separately heterologously expressed in *E. coli* BL21(DE3) and purified by Ni-NTA affinity chromatography. To improve the solubility of the recombinant proteins, PtrCYP97B1 and PtrCYP97B2 were truncated to exclude the N-terminal amino acid residues including the predicted trans-membrane regions or the chloroplast transit peptides. SDS–PAGE analysis showed that PtrCYP97B1 and PtrCYP97B2 were expressed in a soluble form after induction with IPTG (Fig. 5). The recombinant PtrCYP97B1 and PtrCYP97B2 proteins had approximate sizes of 79.64 and 68.28 kDa, respectively. These results suggested that two PtrCYP97Bs enzymes were successful expressed in *E. coli* BL21(DE3).

Functional characterization of PtrCYP97Bs in β-Car-accumulating *E. coli* BL21(DE3) cells In the present study, we used the β-Car-accumulating *E. coli* BL21(DE3) cells to investigate the functions of the two carotene hydroxylase genes (*Ptrcyp97b1* and *Ptrcyp97b2*) of *P. tricornutum* GY-H9. The results showed that only PtrCYP97B2 catalyzed the hydroxylation of the β-rings of β-Car to produce Zea in β-Car-accumulating *E. coli* BL21(DE3) cells, which supported the finding that PtrCYP97B2 might be a key gene for β-Xans accumulation in *P. tricornutum* GY-H9 (Fig. 6A–D,F). It was surprising that only Zea but not β-Cpx was detected. Usually, the

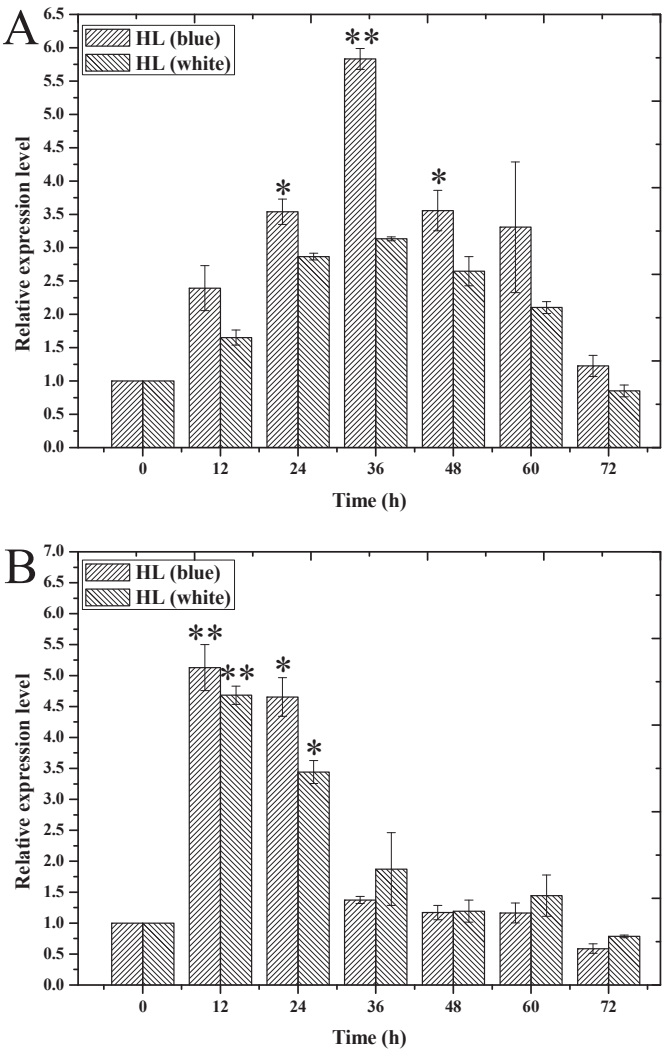

FIG. 3. The mRNA level of *Ptrcyp97b1* and *Ptrcyp97b2* upon white and blue HL conditions. The relative transcript level of *Ptrcyp97b1* (A) and *Ptrcyp97b2* (B) were determined after 12, 24, 36, 48, 60 and 72 h by qRT-PCR using histone as a reference gene. The values were normalized to the transcript level in the normal light condition. *Significantly different at $P < 0.05$; **significantly different at $P < 0.01$.

β-Car may be converted to Zea in vivo by the intermediate metabolite β-Cpx (3,23). Meanwhile the β-Car may also be converted to Vlx in vivo by the intermediate metabolites β-Cpx and β-Cpx-5,6-epoxide (19). However, when PtrCYP97B2 was expressed in β-Car-accumulating *E. coli* BL21(DE3) cells all β-Cpx was further transformed into Zea by the time of the sample was analyzed. In contrast to PtCYP97B2, the carotene hydroxylation activity of PtCYP97B1 was not detected in β-Car-accumulating *E. coli* BL21(DE3) cells (Fig. 6A–E). Therefore, PtrCYP97B1 might be able to catalyze the hydroxylation of other substrates except for β-Car. Further research is needed to test this hypothesis.

DISCUSSION

Previous studies have demonstrated that a Xans cycle (Zea-Atx-Vlx), with Vlx as the putative precursor of Ddx, Dtx and Fcx biosynthesis, was present in *P. tricornutum* (19), which implies that there must be an enzyme that catalyzes the hydroxylation of β-Car. However, the homologous genes of four known types of CHYs (CrtR, BCH, CYP97A and CYP97C) were absent in *P. tricornutum* (2,23). Fortunately, studies have indicated that LUT-like P450 proteins may be responsible for the hydroxylation of Cars in diatoms (23). In addition, two putative genes encoding CYP97Bs (LUT-like1 and LUT-like2) have been predicted in *P. tricornutum* CCAP1055/1 (2,23). Our previous study indicated that *cyp97b* paralogs were present in *P. tricornutum* CCAP1055/1 (2). It is reasonable to speculate that CYP97B may be the possible CHYs in the diatom. To our knowledge, it is the first time that CHYs genes have been isolated and characterized from *P. tricornutum* GY-H9. PtrCYP97B1 and PtrCYP97B2 shared the highest sequences similarity (94/93 %) with the predicted lutein deficient 1-like proteins (LUT-like1 and LUT-like2) in *P. tricornutum* CCAP1055/1 (Table S4). After careful comparative analysis, we think that there are only two genes encoding LUT-like1 and LUT-like2 in *P. tricornutum* CCAP1055/1, which are the two genes most similar to genes of this kind in *P. tricornutum* GY-H9. The isolated PtrCYP97B2 was a chloroplast-targeted protein (Fig. S3), which is consistent with the sub-cellular localization of CYP97A and CYP97C in higher plants and green microalgae and is coincide with the Xans biosynthesis location (16,17,23,30–32). However, PtrCYP97B1 might be a cytoplasm-targeted enzyme encoded by nuclear gene (Fig. S2). The different sub-cellular localization of PtrCYP97B1 and PtrCYP97B2 provides important clues for further functional studies.

CYP450s are defined by the 450 nm light absorption of their heme cofactor and are involved in numerous biosynthetic pathways found in almost all organisms (33). All CYP450s share a common catalytic center, i.e., heme with iron coordinated with the thiolate of a conserved cysteine (34). The CYP450 catalytic motifs were discovered in the protein sequences of PtrCYP97B1 and PtrCYP97B2, indicating that they are two members of the CYP450s family (Fig. 1). In addition, there are some other CYP97B subfamily specific conserved domains (Fig. 1). It is likely that these subfamily specific conserved domains are responsible for the substrate specificity with respect to the β- or ε-ring of the different carotenes (2). At present, gene encoding CYP97 A/B/C subfamily protein from *Arabidopsis* and other land plants is single copy in each organism, which indicating critical function (15). Interesting, in the diatom, there are two genes encoding CYP97Bs building two monophyletic groups. This finding indicates that lineage-specific gene duplication phenomenon may occur before the formation of various algal strains from the diatom (Fig. 2). The Duplication and subsequent functional divergence of genes have been recognized increasingly as an important mechanism of evolution (2,35).

Light is considered an effective stimulus for inducing carotenoids biosynthesis related genes expression and accumulation in *P. tricornutum* (23,36–38). Our results suggested that *Ptrcyp97b1* and *Ptrcyp97b2* transcription was mainly influenced by different HL conditions. As shown in Fig. 3, the responses of both *Ptrcyp97b1* and *Ptrcyp97b2* genes began 12 h later under HL conditions in this study, which is not consistent with the short respond time (2–6 h) of *psy*, *pds*, *zep1*, *zep2*, *zep3*, *vde*, *vdl1* and *vdl2* genes under white or blue HL conditions (23). One possible reason for above phenomenon is the missing sampling time points from 0 to 12 h. In addition, continuous respond over time (12–60 h) is the characteristic for *Ptrcyp97b1*. However, transitory respond short time (12–24 h) is the prototypical properties for *Ptrcyp97b2* which is similar with other CHYs (*Haecyp97a*, *Haecyp97b*, *Haecyp97c* and *Ckecyp97a*) in *Haematococcus pluvialis* and *Chlorella kessleri* under both white and blue HL conditions (2,16,17). The distinct kinetics of increase for *Ptrcyp97b1* and *Ptrcyp97b2* under different HL conditions implied that they have various function. Moreover, our results indicated that blue HL is more effective for inducing the expression of *Ptrcyp97b1* and *Ptrcyp97b2* than white HL stress. This phenomenon is similar to that found in our previous studies which indicated that blue HL is more effective for inducing the expression of *Haebch*, *Haecyp97a* and *Haecyp97c* and the accumulation of astaxanthin in *H. pluvialis* (2,16). Generally, blue light can be absorbed almost

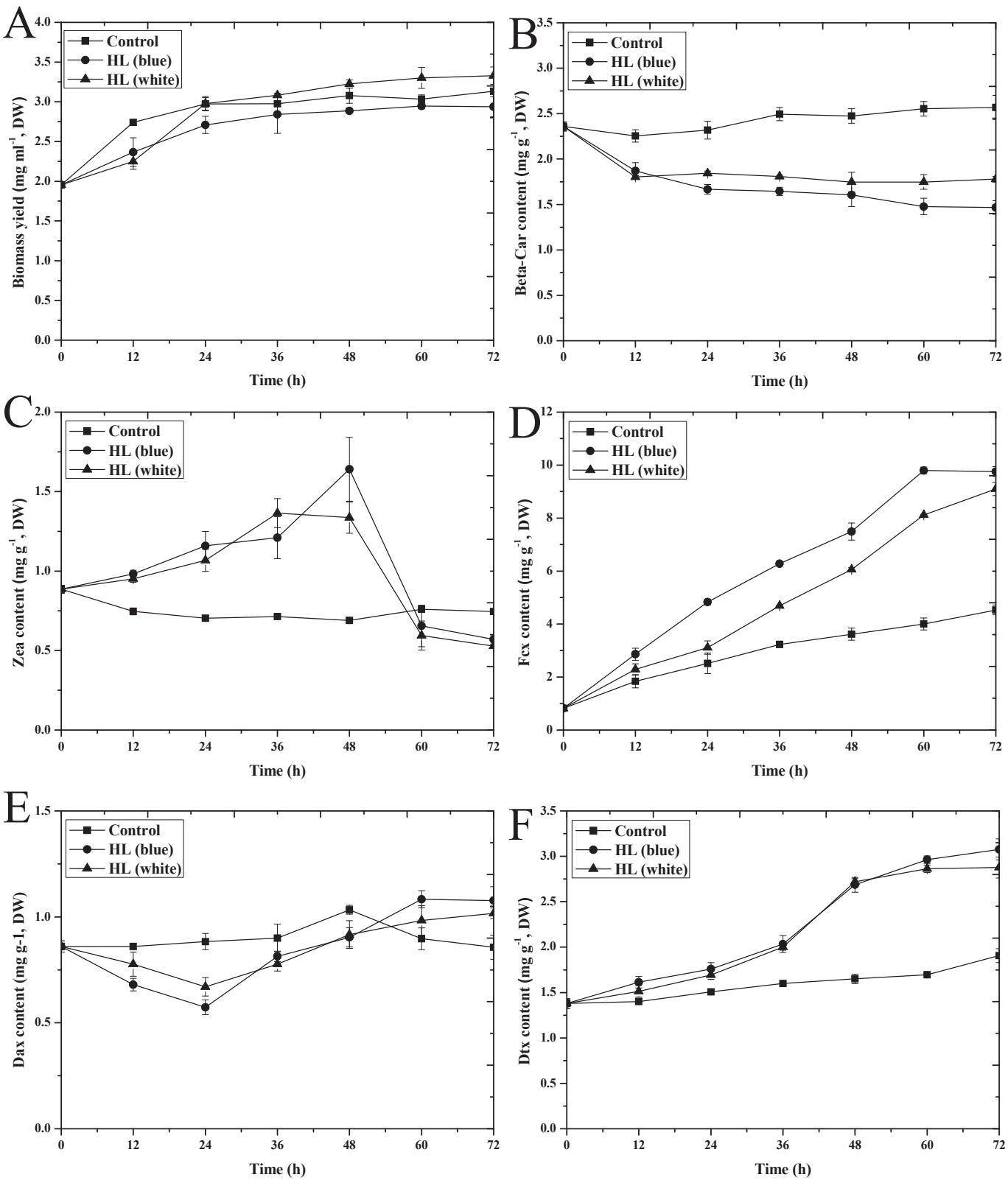

FIG. 4. The growth and contents of β-Car, Zea, Fcx Ddx and Dtx upon white and blue HL conditions. The biomass yield of *P. tricornutum* GY-H9 (A), the content of β-Car (B), the content of Zea (C), the content of Fcx (D), the content of Ddx (E) and the content of Dtx (F) were determined after 12, 24, 36, 48, 60 and 72 h. The values were normalized to the level in the normal light condition.

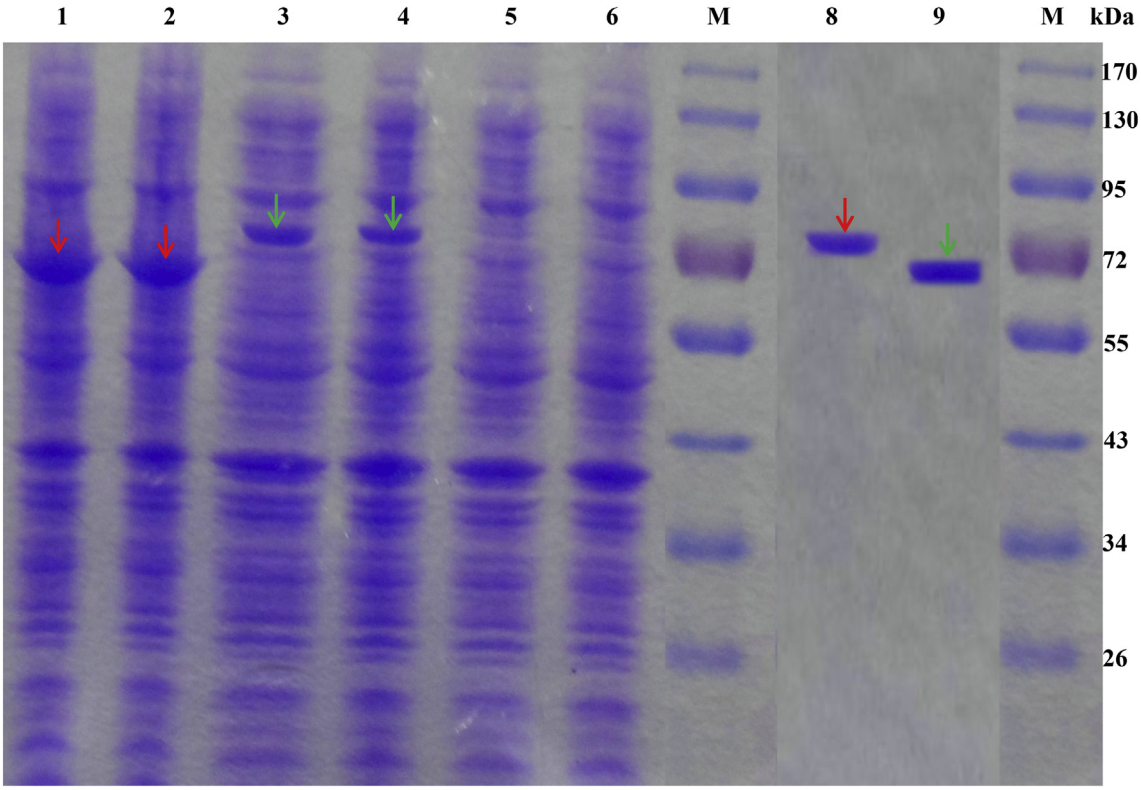

FIG. 5. SDS–PAGE and purification of recombinant PtrCYP97B1 and PtrCYP97B2. Lane M, molecular weight markers; lanes 1 and 2, PtrCYP97B1 expression induced in *E. coli* BL21 by IPTG at 6 h and 24 h; lanes 3 and 4, PtrCYP97B2 expression induced in *E. coli* BL21 by IPTG at 6 h and 24 h; lanes 5 and 6, empty plasmid expression induced in *E. coli* BL21 by IPTG at 6 h and 24 h; lanes 8 and 9, the recombinant PtrCYP97B1 and PtrCYP97B2 purified through Ni-chelating affinity chromatography. The PtrCYP97B1 and PtrCYP97B2 target proteins were indicated by red arrow and green arrow, respectively.

completely, whereas this is not the case for white light. Therefore, under the same amounts of photons of white and blue light, blue light constitutes more of a HL condition than white light (39). In addition, previous studies have shown that blue light is essential for HL acclimation in the marine diatom *P. tricornutum*. Light acclimation is a complex process mediated by blue light receptor aureochrome or photoreceptor-triggered transcription factors (40). Total 7193 genes (58% of all genes) were significantly differentially regulated by plant-like cryptochrome under blue HL condition in *P. tricornutum* (41). Thus, blue light had a more up-regulating effect on gene expression (41). According to above results, we speculate that carotenoids biosynthetic genes expression for *P. tricornutum* depends on not only light intensity, but also light quality. In this present study, for HL conditions, the later exponentially growing cells were further used to investigate the effects of different HL light conditions. Under the circumstances, the nutrient limitation and cell status might play an important role besides high light stress. Previous studies have indicated that nitrogen limitation inhibits the growth and produces marked changes in biochemical composition including an increases the lipid amount and decreases the biomass and chlorophyll *a*, total carotenoids and protein of the cells (42,43).

The major carotenoids were analyzed based on the HPLC method. As shown in Fig. 4. The β-Car, Zea, Fcx, Dtx and Ddx were the main carotenoids in *P. tricornutum*. In our studies, the β-Cpx, β-Cpx-epoxide,Vlx and Atx were not detected, which is not consistent with recently studies (44). We assume that the level of these Xans may be low and not detectable on this HPLC method used in our study. In our study, both blue and white HL conditions decreased the content of β-Car and increased the contents of Fcx and Dtx. The direct intermediate metabolite Zea increased in early induction and decreased sharply in later induction (Fig. 4). These results are not consistent with previous studies that indicated that the accumulation of Fcx was promoted under red light and green light. Blue light inhibited the growth and biosynthesis of Fcx in *P. tricornutum* (38). In general, cells seem to react quickly to the increase in light intensity. For instance, the contents of Ddx and Dtx increased dramatically after 6–24 h and increased steadily during 24–72 h and reached its maximum (3.4-fold) on the 72 h under sine HL (500 μmol photons m^{-2} s^{-1}) condition in four strains of *P. tricornutum* (CCAP1055/1, Pt1sil, Pt4 and Pt4ov) (45). However, under fluctuating HL (500 or 1000 μmol photons m^{-2} s^{-1}) condition, the increase of Ddx and Dtx pigments was only 1.7-fold higher than the control at the last time 72 h and a trend of slow increase was observed (45). In our results, although the maximal contents of Dtx and Fcx were reached at last time (72 h), a trend of slow increase was also observed in the early stress induction (0–36 h), which was similar with the previous results from *P. tricornutum* under fluctuating HL condition. In addition, the later exponentially growing cells were used to investigate the effects of different HL conditions in this study. Under the circumstances, the nutrient limitation and cell status might play an important role besides HL stress. Therefore, the physiological state of cells (i.e., cells reach stationary phase) and the pattern of HL (light quality, light intensity, light model and photoperiod) may be responsible for this phenomenon. According to the results from transcriptional expression of *Ptrcyp97*bs genes and carotenoids accumulation of Xans under HL conditions, it is reasonable to speculate that the PtrCYP97B1 and PtrCYP97B2 enzymes may co-involve in Xans biosynthesis by hydroxylation of β-Car into intermediate metabolite Zea, which testified the previous predicted biosynthetic pathway (3,23).

Usually, *E. coli* cells accumulating different carotenoids have been identified to be an efficient platform for investigating the functions of algal carotenoid metabolic genes (46–49). In the

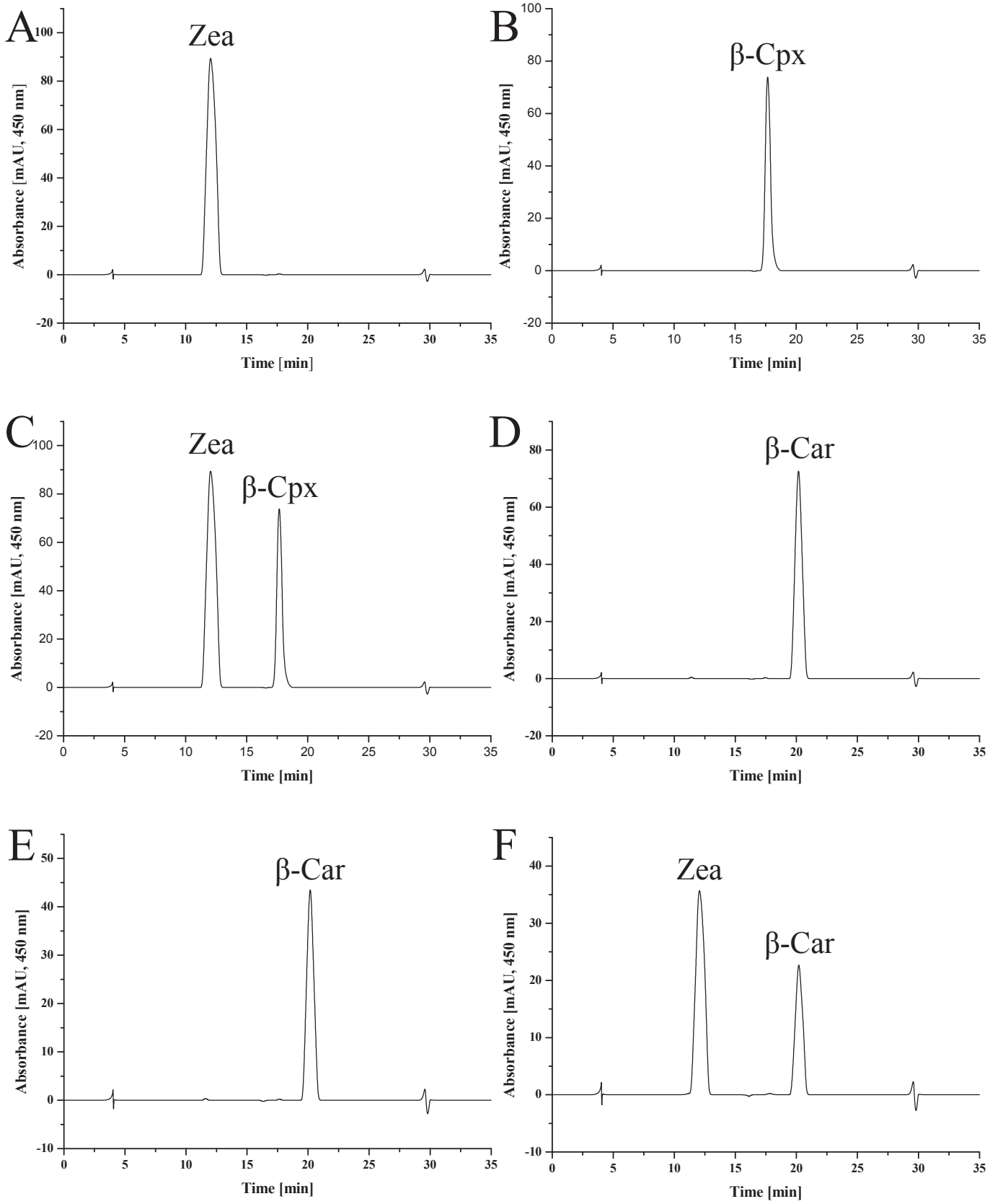

FIG. 6. HPLC analysis of carotenoids in β-carotene-accumulating *E. coli* BL21(DE3) cells. The Zea standard (A), the β-Cpx standard (B), the Zea and β-Cpx standards (C), the *E. coli* BL21(DE3) cells harboring pACCAR16ΔcrtX (D), the *E. coli* BL21(DE3) cells harboring pACCAR16ΔcrtX and pET-28a (+)-*Ptrcyp97b1* (E), the *E. coli* BL21(DE3) cells harboring pACCAR16ΔcrtX and pET-28a (+)-*Ptrcyp97b2* (F).

TMHMM analysis of PtrCYP97Bs, an N-terminal trans-membrane region from Met-1 to Ser-62 was predicted in PtrCYP97B1 (Fig. S2). In the signal peptides analysis for the PtrCYP97Bs, an N-terminal chloroplast transit peptides region from Met-1 to Pro-28 was predicted in PtrCYP97B2 (Fig. S3). Previous studies have reported that deletion of the N-terminal trans-membrane segment of NADPH-dependent cytochrome P450 reductase in green microalgae enabled the high expression of the soluble recombinant protein (46). Since the full-length cDNA sequences of *Ptrcyp97b1* and *Ptrcyp97b2* were not successfully expressed in *E. coli* (data not shown), the same technique was applied in this study. The truncated PtrCYP97B1 and PtrCYP97B2 were successfully heterologously expressed in *E. coli* as soluble and functional proteins (Fig. 5). The functional analysis results showed that PtrCYP97B2 could catalyze the hydroxylation of the β-rings of β-Car to produce Zea in β-Car-accumulating *E. coli* BL21(DE3) cells (Fig. 6). It is surprising that only Zea but not β-Cpx was detected, this finding might be interpreted to mean that all the β-Cpx was transformed into Zea by the time of the *E. coli* BL21(DE3) cells were analyzed. Moreover, the carotene hydroxylation activity of PtrCYP97B1 was not detected in β-Car-accumulating *E. coli* BL21(DE3) cells (Fig. 6), which indicated that PtrCYP97B1 might be able to catalyze the hydroxylation of other substrates except for β-Car. The *E. coli* BL21(DE3) cells that accumulate other carotenoids (e.g., α-Car) should be used for further investigation into the function of PtrCYP97B1. The functions of CYP97 A/B/C members are various and species-specific. In higher plants (*Arabidopsis* and rice), it was reported that CYP97A could hydroxylase β-rings of β-Car to produce β-Cpx and Zea in turn. Meanwhile, it is mainly responsible for the hydroxylation of β-ring of α-Car to produce zeinoxanthin, and then zeinoxanthin was further hydroxylated by CYP97C to produce lutein (31). However, in *Satsuma mandarin*, CitBCH and CitCYP97C were participated in the biosynthesis of lutein (47). The carotene hydroxylation activities of CitCYP97A and CitCYP97B were not detected in β-Car-accumulating *E. coli* BL21(DE3) cells (48). To date, few CYP97B genes have been functionally characterized. Fortunately, the hydroxylation of the β-rings of β-Car to produce Zea was detected, which is consistent with the function of CYP97B (PuCHY1) from red algae (*Porphyra*) (22). Although it is difficult to completely understand the functions of the two PtrCYP97Bs in vivo and in vitro, we supply two candidate genes encoding CYP97Bs involved in the hydroxylation of β-Car. This study provides information on gene cloning and functional investigation of CYP97Bs in *P. tricornutum* in the future. In addition, over-expression and knock-down of the two *Ptrcyp97b1* and *Ptrcyp97b2* genes are necessary to elaborate the true function of *P. tricornutum* in vivo. Although carotene hydroxylation is the crucial step in the Fcx upstream biosynthetic pathway but is not a direct step in its production (3,19,23). The downstream biosynthetic pathway of Fcx in *P. tricornutum* seems to be very complicated and requires additional enzymes including PtrVDE, PtrDDE, PtrVDL1, PtrVDL2, PtrZEP-1, PtrZEP-2 and PtrZEP-3 (14,50,51). The further synthetic biology studies focusing on assembling these genes to create new metabolic pathways in β-Car-accumulating *E. coli* BL21(DE3) are expected to be powerful tools for uncovering the Fcx biosynthesis pathway.

Supplementary data to this article can be found online at https://doi.org/10.1016/j.jbiosc.2019.06.008.

ACKNOWLEDGMENTS

This work was supported by China Postdoctoral Science Foundation (Grant No. 2018M631768), Science and Technology Planning Project of Liaoning Province (Grant No. 20170540047), Applying Basic Research Planning Project of Shanxi Province (Science and Technology Foundation for Youths) (Grant No. 201801D221250), Key Research and Development (R&D) Planning Project of Shanxi Province (Grant No. 201803D31063), The State Ministry of Agriculture "948" Project (2014-Z39), Shanxi Province Key Projects of Coal-based Science and Technology (FT-2014-01), Research Project Supported by Shanxi Scholarship Council of China (2015-064), and the Key Project of the Key Research and Development Program of Shanxi Province, China (Grant No. 201603D312005).

References

1. **Dambek, M., Eilers, U., Breitenbach, J., Steiger, S., Büchel, C., and Sandmann, G.:** Biosynthesis of fucoxanthin and diadinoxanthin and function of initial pathway genes in *Phaeodactylum tricornutum*, J. Exp. Bot., **63**, 5607–5612 (2012).
2. **Cui, H. L., Yu, X. N., Yan, W., Cui, Y. L., Li, X. Q., Liu, Z. P., and Qin, S.:** Evolutionary origins, molecular cloning and expression of carotenoid hydroxylases in eukaryotic photosynthetic algae, BMC Genomics, **14**, 457 (2013).
3. **Gong, M. and Bassi, A.:** Carotenoids from microalgae: a review of recent developments, Biotechnol. Adv., **34**, 1396–1412 (2016).
4. **Raposo, M. F., de Morais, A. M., and de Morais, R. M.:** Carotenoids from marine microalgae: a valuable natural source for the prevention of chronic diseases, Mar. Drugs, **13**, 5128–5155 (2015).
5. **Schaller-Laudel, S., Volke, D., Redlich, M., Kansy, M., Hoffmann, R., Wilhelm, C., and Goss, R.:** The diadinoxanthin diatoxanthin cycle induces structural rearrangements of the isolated FCP antenna complexes of the pennate diatom *Phaeodactylum tricornutum*, Plant Physiol. Biochem., **96**, 364–376 (2015).
6. **Peng, J., Yuan, J. P., Wu, C. F., and Wang, J. H.:** Fucoxanthin, a marine carotenoid present in brown seaweeds and diatoms: metabolism and bioactivities relevant to human health, Mar. Drugs, **9**, 1806–1828 (2011).
7. **Kim, K. N., Heo, S. J., Yoon, W. J., Kang, S. M., Ahn, G., Yi, T. H., and Jeon, Y. J.:** Fucoxanthin inhibits the inflammatory response by suppressing the activation of NF-κB and MAPKs in lipopolysaccharide-induced RAW 264.7 macrophages, Eur. J. Pharmacol., **649**, 369–375 (2010).
8. **Pai-An, H., Nhut, P. N., Lu, W. J., Thi, N. H. B., and Lin, Y. C.:** Low-molecular-weight fucoidan and high-stability fucoxanthin from brown seaweed exert prebiotics and anti-inflammatory activities in Caco-2 cells, Food Nutr. Res., **60**, 32033 (2016).
9. **Seo, M. J., Seo, Y. J., Pan, C. H., Lee, O. H., Kim, K. J., and Lee, B. Y.:** Fucoxanthin suppresses lipid accumulation and ROS production during differentiation in 3T3-L1 adipocytes, Phytother Res., **30**, 1802–1808 (2016).
10. **Su, C. F., Yusoff, F. M., Ismail, M., Basri, M., Yau, S. K., Khong, N. M. H., Chan, K. W., and Ebrahimi, M.:** Antioxidant capacities of fucoxanthin producing algae as influenced by their carotenoid and phenolic contents, J. Biotechnol., **241**, 175–183 (2016).
11. **Mei, C. H., Zhou, S. C., Lin, Z., Ming, J. X., Zeng, F. D., and Xu, R.:** Antitumor effects of laminaria extract fucoxanthin on lung cancer, Mar. Drugs, **15**, 39 (2017).
12. **Sang, M. K., Jung, Y. J., Kwon, O. N., Cha, K. H., Um, B. H., Chung, D., and Pan, C. H.:** A potential commercial source of fucoxanthin extracted from the microalga *Phaeodactylum tricornutum*, Appl. Biochem. Biotechnol., **166**, 1843–1855 (2012).
13. **Bowler, C., Allen, A. E., Badger, J. H., Grimwood, J., Jabbari, K., Kuo, A., Maheswari, U., Martens, C., Maumus, F., Otillar, R. P., and other 67 authors:** The *Phaeodactylum* genome reveals the evolutionary history of diatom genomes, Nature, **456**, 239–244 (2008).
14. **Eilers, U., Bikoulis, A., Breitenbach, J., Büchel, C., and Sandmann, G.:** Limitations in the biosynthesis of fucoxanthin as targets for genetic engineering in *Phaeodactylum tricornutum*, J. Appl. Phycol., **28**, 123–129 (2016).
15. **Kim, J., Smith, J. J., Tian, L., and Dellapenna, D.:** The evolution and function of carotenoid hydroxylases in *Arabidopsis*, Plant Cell Physiol., **50**, 463–479 (2009).
16. **Cui, H. L., Yu, X. N., Wang, Y., Cui, Y. L., Li, X. Q., Liu, Z. P., and Qin, S.:** Gene cloning and expression profile of a novel carotenoid hydroxylase (CYP97C) from the green alga *Haematococcus pluvialis*, J. Appl. Phycol., **26**, 91–103 (2014).
17. **Yu, X. N., Cui, H. L., Cui, Y. L., Wang, Y., Li, X. Q., Liu, Z. P., and Qin, S.:** Gene cloning, sequence analysis, and expression profiles of a novel β-ring carotenoid hydroxylase gene from the photoheterotrophic green alga *Chlorella kessleri*, Mol. Biol. Rep., **41**, 7103–7113 (2014).
18. **Makino, T., Harada, H., Ikenaga, H., Matsuda, S., Takaichi, S., Shindo, K., Sandmann, G., Ogata, T., and Misawa, N.:** Characterization of cyanobacterial carotenoid ketolase CrtW and hydroxylase CrtR by complementation analysis in *Escherichia coli*, Plant Cell Physiol., **49**, 1867–1878 (2008).
19. **Bertrand, M.:** Carotenoid biosynthesis in diatoms, Photosynth. Res., **106**, 89–102 (2010).
20. **Kim, J. E., Cheng, K. M., Craft, N. E., Hamberger, B., and Douglas, C. J.:** Over-expression of *Arabidopsis thaliana* carotenoid hydroxylases individually and in

combination with a β-carotene ketolase provides insight into in *vivo* functions, Phytochemistry, **71**, 168–178 (2010).
21. **Dall'Osto, L., Holt, N. E., Kaligotla, S., Fuciman, M., Cazzaniga, S., Carbonera, D., Frank, H. A., Alric, J., and Bassi, R.:** Zeaxanthin protects plant photosynthesis by modulating chlorophyll triplet yield in specific light-harvesting antenna subunits, J. Biol. Chem., **287**, 41820–41834 (2012).
22. **Yang, L. E., Huang, X. Q., Huang, Y., Deng, Y. Y., Lu, Q. Q., and Lu, S.:** The P450-type carotene hydroxylase PuCHY1 from *Porphyra* suggests the evolution of carotenoid metabolism in red algae, J. Integr. Plant Biol., **56**, 902–915 (2014).
23. **Coesel, S., Oborník, M., Varela, J., Falciatore, A., and Bowler, C.:** Evolutionary origins and functions of the carotenoid biosynthetic pathway in marine diatoms, PLoS One, **3**, e2896 (2008).
24. **Bordoli, L., Kiefer, F., Arnold, K., Benkert, P., Battey, J., and Schwede, T.:** Protein structure homology modeling using SWISS-MODEL workspace, Nat. Protoc., **4**, 1–13 (2009).
25. **Larkin, M. A., Blackshields, G., and Brown, N. P.:** ClustalW and clustal X version 2, Bioinformatics, **23**, 2947–2948 (2007).
26. **Le, S. Q. and Gascuel, O.:** An improved general amino acid replacement matrix, Mol. Biol. Evol., **25**, 1307–1320 (2008).
27. **Guindon, S., Dufayard, J. F., Hordijk, W., Lefort, V., and Gascuel, O.:** Phyml: fast and accurate phylogeny reconstruction by maximum likelihood, Infect. Genet. Evol., **9**, 384–385 (2009).
28. **Rao, X., Huang, X., Zhou, Z., and Lin, X.:** An improvement of the $2^{-(\text{-delta delta CT})}$ method for quantitative real-time polymerase chain reaction data analysis, Biostat. Bioinforma. Biomath., **3**, 71–85 (2013).
29. **G Misawa, N., Kajiwara, S., Kondo, K., Yokoyama, A., Satomi, Y., Saito, T., Miki, W., and Ohtani, T.:** Canthaxanthin biosynthesis by the conversion of methylene to keto groups in a hydrocarbon β-carotene by a single gene, Biochem. Biophys. Res. Commun., **209**, 867–876 (1995).
30. **Kim, J. and Dellapenna, D.:** Defining the primary route for lutein synthesis in plants: the role of *Arabidopsis* carotenoid β-ring hydroxylase CYP97A3, Proc. Natl. Acad. Sci. USA, **103**, 3474–3479 (2006).
31. **Lv, M. Z., Chao, D. Y., Shan, J. X., Zhu, M. Z., Shi, M., Gao, J. P., and Lin, H. X.:** Rice carotenoid β-ring hydroxylase CYP97A4 is involved in lutein biosynthesis, Plant Cell Physiol., **53**, 987–1002 (2012).
32. **Tian, L. and Dellapenna, D.:** Progress in understanding the origin and functions of carotenoid hydroxylases in plants, Arch. Biochem. Biophys., **430**, 22–29 (2004).
33. **Nelson, D. and Werck-Reichhart, D.:** A P450-centric view of plant evolution, Plant J., **66**, 194–211 (2011).
34. **Werckreichhart, D. and Feyereisen, R.:** Cytochromes P450: a success story, Genome Biol., **1**, 1–9 (2000).
35. **Lan, T. T., Taylor, J. S., and Constabel, C. P.:** The polyphenol oxidase gene family in land plants: lineage-specific duplication and expansion, BMC Genomics, **13**, 395 (2012).
36. **Schellenberger, C. B., Jungandreas, A., Jakob, T., Weisheit, W., Mittag, M., and Wilhelm, C.:** Blue light is essential for high light acclimation and photoprotection in the diatom *Phaeodactylum tricornutum*, J. Exp. Bot., **64**, 483–493 (2013).
37. **Yi, Z. Q., Xu, M. N., Magnusdottir, M., Zhang, Y. T., Brynjolfsson, S., and Fu, W. Q.:** Photo-oxidative stress-driven mutagenesis and adaptive evolution on the marine diatom *Phaeodactylum tricornutum* for enhanced carotenoid accumulation, Mar. Drugs, **13**, 6138–6151 (2015).
38. **Gómez-Loredo, A., Benavides, J., and Rito-Palomares, M.:** Growth kinetics and fucoxanthin production of *Phaeodactylum tricornutum* and *Isochrysis galbana* cultures at different light and agitation conditions, J. Appl. Phycol., **28**, 849–860 (2016).
39. **Glover, H. E., Keller, M. D., and Spinrad, R. W.:** The effects of light quality and intensity on photosynthesis and growth of marine eukaryotic and prokaryotic phytoplankton clones, J. Exp. Mar. Biol. Ecol., **105**, 137–159 (1987).
40. **Mann, M., Serif, M., Jakob, T., Kroth, P. G., and Wilhelm, C.:** PtAUREO1a and PtAUREO1b knockout mutants of the diatom *Phaeodactylum tricornutum* are blocked in photoacclimation to blue light, J. Plant Physiol., **217**, 44–48 (2017).
41. **Konig, S., Eisenhu, M., Brautigam, A., Kurz, S., Weber, A. P. M., and Buchel, C.:** The influence of a cryptochrome on the gene expression profile in the diatom *Phaeodactylum tricornutum* under blue light and in darkness, Plant Cell Physiol., **58**, 1914–1923 (2017).
42. **Burcu, A. K., Oya, I., Uslu, L., and Azgın, C.:** The effect of stress due to nitrogen limitation on lipid content of *Phaeodactylum Tricornutum* (Bohlin) cultured outdoor in photobioreactor, Turk. J. Fish. Aquat. Sci., **15**, 647–652 (2015).
43. **Osborne, B. and Geider, R. J.:** Effect of nitrate-nitrogen limitation on photosynthesis of the diatom *Phaeodactylum tricornutum* Bohlin (Bacillariophyceae), Plant Cell Environ., **9**, 617–625 (2010).
44. **Kuczynska, P. and Jemiola-Rzeminska, M.:** Isolation and purification of all-*trans* diadinoxanthin and all-*trans* diatoxanthin from diatom *Phaeodactylum tricornutum*, J. Appl. Phycol., **29**, 79–87 (2017).
45. **Tsou, C. Y., Matsunaga, S., and Okada, S.:** Molecular cloning and functional characterization of NADPH-dependent cytochrome P450 reductase from the green microalga *Botryococcus braunii*, B race, J. Biosci. Bioeng., **125**, 30–37 (2018).
46. **Huang, J. C., Wang, Y., Sandmann, G., and Chen, F.:** Isolation and characterization of a carotenoid oxygenase gene from *Chlorella zofingiensis* (Chlorophyta), Appl. Microbiol. Biotechnol., **71**, 473–479 (2006).
47. **Gang, M., Zhang, L., Witchulada, Y., Issei, T., Natsumi, I., Michiru, O., Kazuki, Y., Masaki, Y., and Masaya, K.:** Expression and functional analysis of citrus carotene hydroxylases: unravelling the xanthophyll biosynthesis in citrus fruits, BMC Plant Biol., **16**, 148 (2016).
48. **Lao, Y. M., Jin, H., Zhou, J., Zhang, H. J., and Cai, Z. H.:** Functional characterization of a missing branch component in *Haematococcus pluvialis* for control of algal carotenoid biosynthesis, Front. Plant Sci., **8**, 1341 (2017).
49. **Lavaud, J., Materna, A. C., Sturm, S., Vugrinec, S., and Kroth, P. G.:** Silencing of the violaxanthin de-epoxidase gene in the diatom *Phaeodactylum tricornutum* reduces diatoxanthin synthesis and non-photochemical quenching, PLoS One, **7**, e36806 (2012).
50. **Bojko, M., Olchawa-Pajor, M., Tuleja, U., Kuczyńska, P., Strzałka, W., Latowski, D., and Strzałka, K.:** Expression of three diadinoxanthin de-epoxidase genes of *Phaeodacylum tricornutum* in *Escherichia coli Origami b* and BL21 strain, Acta Biochim. Pol., **60**, 857–860 (2013).
51. **Lepetit, B., Gelin, G., Lepetit, M., Sturm, S., Vugrinec, S., Rogato, A., Kroth, P. G., Falciatore, A., and Lavaud, J.:** The diatom *Phaeodactylum tricornutum* adjusts nonphotochemical fluorescence quenching capacity in response to dynamic light via fine-tuned Lhcx and xanthophyll cycle pigment synthesis, New Phytol., **214**, 205–218 (2017).